ACS APPLIED MATERIALS & INTERFACES

Research Article

www.acsami.org

Directed Assembly of Nanodiamond Nitrogen-Vacancy Centers on a Chemically Modified Patterned Surface

Saleem G Rao,*[,†] Altaf Karim,[‡,○] Julian Schwartz,[§,∥] Natania Antler,[⊥] Thomas Schenkel,[∥] and Irfan Siddiqi[⊥]

[†]Department of Physics, King Fahd University of Petroleum and Minerals, Dhahran 31261, Saudi Arabia

[‡]Enviornmental Energy Technologies Division and [∥]Accelerator and Fusion Research Division, Lawrence Berkeley National Laboratory, Berkeley, California 94720, United States

[§]Department of Micro- and Nanoelectronical Systems, Institute of Micro- and Nanoelectronics, Technical University Ilmenau, PF 10 05 65, 98684 Ilmenau, Germany

[⊥]Department of Physics, Quantum Nanoelectronics Laboratory, University of California, Berkeley, California 94709, United States

Supporting Information

ABSTRACT: Nitrogen-vacancy (NV) centers in nanodiamond (ND) particles are an attractive material for photonic, quantum information, and biological sensing technologies due to their optical properties—bright single photon emission and long spin coherence time. To harness these features in practical devices, it is essential to realize efficient methods to assemble and pattern NDs at the micro-/nanoscale. In this work, we report the large scale patterned assembly of NDs on a Au surface by creating hydrophobic and hydrophilic regions using self-assembled monolayer (SAM). Hydrophobic regions are created using a methyl ($-CH_3$) terminated SAM of octadecanethiol molecules. Evaporating a water droplet suspension of NDs on the SAM patterned surface assembles the NDs in the bare Au, hydrophilic regions. Using this procedure, we successfully produced a ND structures in the shape of dots, lines, and rectangles. Subsequent photoluminescence imaging of the patterned NDs confirmed the presence of optically active NV centers. Experimental evidence in conjunction with computational analysis indicates that the surface wettability of the SAM modified Au surface plays a dominant role in the assembly of NDs as compared to van der Waals and other substrate−ND interactions.

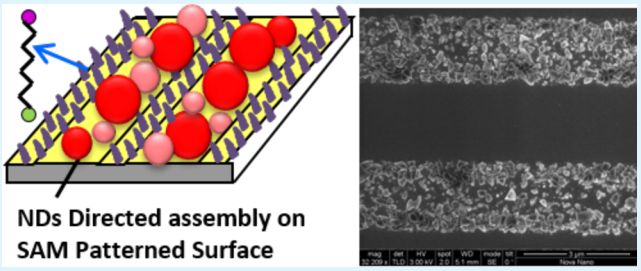

KEYWORDS: *nitrogen-vacancy center nanodiamond, directed self-assembly, self-assembled monolayer*

1. INTRODUCTION

The miniaturization of electronic and optical circuits to the nanoscale has established new paradigms for information processing and sensing. In analogy to the single electron transistor,[1,2] magnetic and optical devices have also been scaled down and operate with single quantum sensitivity, helping drive the active research fields of spintronics[3] and nanophotonics.[4,5] Recently important steps have been made in the design and fabrication of efficient and bright solid-state single photon sources.[6] Such sources are of particular interest to build quantum information devices and to realize quantum cryptography. Nitrogen-vacancy (NV) centers in diamond[7] are particularly attractive because of individual addressability,[8] optical spin polarization, and millisecond room-temperature spin coherence.[9] These properties have generated intense interest in the use of NV centers for quantum device applications in dipolar-coupled quantum registers[10] and hybrid quantum computing architectures[11,12] in addition to magnetometery, biolabeling, drug delivery, and subdiffraction optical imaging.[13] An outstanding challenge, however, to using NV centers in complex devices such as an array of quantum bits in an electronic circuit, NV centers coupled to optical microcavity resonators, or magnetometers, is their spatial manipulation at micro-/nanoscale. Many different fabrication techniques for NV devices in bulk diamond[13] and diamond nanocrystals[14] have been reported.

Among the different methods used to produce functional NV devices, there is the statistical, random assembly approach, self-assembly (due to interparticle interactions), directed self-assembly (seed growth and field guided assembly),[15] and the directed growth of photonic crystals or quantum dots around each other.[16,17] For NDs in particular, bottom up scanning probe "pick and place" assembly[14] has been effectively employed whereas the generation of a matrix of active NV centers, with and without lithographic patterning,[13] is commonplace in top down fabrication. Recently top down nanofabrication has been shown to provide a reliable and high-throughput means to generate large array of photonic devices.[18] However, synthesis

Received: May 9, 2014
Accepted: July 16, 2014
Published: July 16, 2014

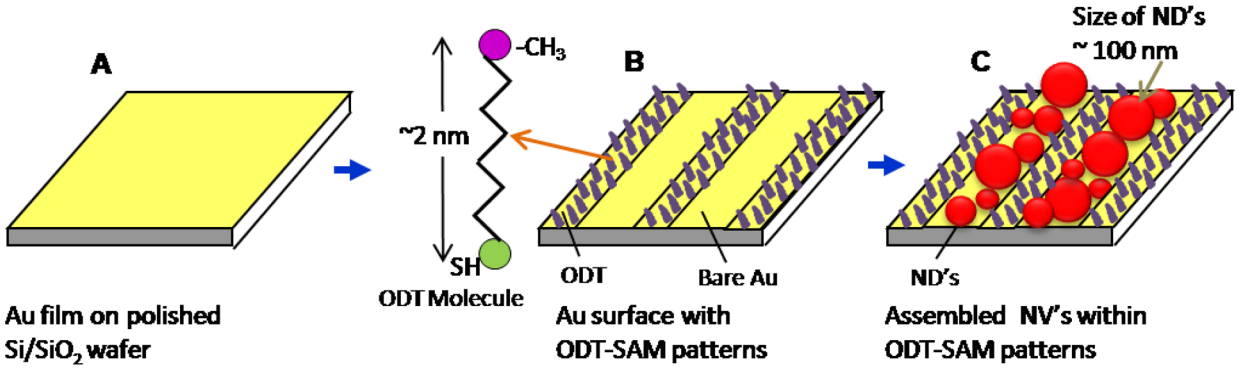

Figure 1. Schematic diagram depicting the procedure to assemble and pattern the NDs on a SAM modified Au surface. (A) Au thin film on Si/SiO_2 substrate. (B) ODT-SAM patterned Au surface. (C) Assembled NDs on bare Au surface between ODT-SAM patterns.

via nanostructures (NS) offers the potential of fabrication in less time, at low cost, with high yield, and without the need for ultrahigh vacuum. Optically active NV centers can be readily created by exposing diamond nanoparticles/powder/dust to a high-energy ion beam,[19] and this starting material can then be distributed to multiple users for integration into complex devices, given the availability of robust patterning techniques. Though current bottom up approaches based on scanning probe "pick and place" methods are an option, they typically are characterized by low yield and slow, serial processing.

Here we report a simple and high yield bottom up approach to assemble NDs over large areas using a chemically modified surface. In this process hydrophobic and hydrophilic regions are created on a Au surface using methyl ($-CH_3$) terminated octadecanethiol (ODT) SAMs. By letting a droplet of ND in water suspension evaporate on the SAM patterned surface, we observe the selective deposition of NDs in the bare Au (hydrophilic) regions. ODT SAM patterns were used to create basic geometric structures such as lines, dots and rectangular regions of NDs on the bare Au surface. The number of NDs in each bare Au region depends upon the concentration of NDs in droplet and the size of the region. SAM assisted patterning has been reported in the literature for a variety of NSs where columbic interaction,[20−23] interaction between the NS and the substrate (with and without SAM modification), and the relative energies of the NS in solvent versus on the substrate,[24] play an important role in the assembly process. According to recent reports, controlled solvent evaporation mediated by topographic features[25−27] and by controlled evaporation "coffee rings"[28−30] can be used to assemble NS in some specific geometries. Moreover, solvent surface wettability effects in patterned assembly of carbon nanotubes (CNTs) and nanoparticles have been reported[31−34] in addition to assembly on physical templated surface due to capillary forces in fluidic cell[35] and others.[36] Much in the spirit of these previous works, our experiments with patterned ND assembly also indicate that surface wettability, controlled via the deposition of a SAM pattern, plays a key role in the assembly process and allows us to assemble NDs with a high degree of flexibility with respect to device geometry. Furthermore, our computational model for ND assembly suggests that solvent evaporation dynamics are dominant in the assembly process. Thus, this type of bottom up approach gives a new and simple solution for patterning NDs at large scale and is compatible with standard semiconductor fabrication—an advantage for producing integrated nanophotonic devices.

2. EXPERIMENTAL METHODS

Figure 1 is a schematic diagram illustrating the ND assembly and patterning procedure investigated in this work. First, a thin gold film is created by depositing Cr/Au (5 nm/20 nm) on a Si/SiO_2 substrate using thermal evaporation system (Figure1A). Next, a micrometer scale pattern of ODT (Sigma-Aldrich, 2 mM solution in ethanol) SAM stripes on the Au film is created using microcontact printing (Figure 1B). Square and rectangular SAM patterns (of ODT) were created in the same way. The thiol (−SH) termination of the ODT (green circles) binds with the Au surface while the methyl ($-CH_3$) end (purple circles) remains free, thus rendering the patterned regions hydrophobic. The methyl-terminated end of the ODT prevents the NDs from binding due to a reduction in wettability. Commercially available (International Technology Center) carboxylated NDs suspended in 0.1 wt % water with an average size of 100 nm were used in this study. A drop of the NDs suspension was placed on the SAM patterned surface and allowed to dry. As the solvent evaporates, it leaves behind NDs in the bare Au regions, as defined by the SAM pattern (Figure 1C)

Images of the sample were then taken by both an optical microscope (Olympus-BX60MFS) with an Infinity2 CCD camera and a scanning electron microscope (FEI Nova Nano SEM). Photoluminescence (PL) images, at different intensities, were taken with a Horiba Scientific LabRAM ARAMIS confocal microscope, 532 nm excitation wavelength laser, 100× objectives, and with full spectral resolution. These 2D images were generated from the intensity of the spectra from 635−642 nm. The crystalline structure of the NDs was characterized by Shimadzu XRD Model 6000 using an X-ray source with Cu−Kα wavelength at λ = 1.54 Å.

For the computational model, we calculated the diffusion barriers ($\Delta E_{diff,i}$) for the NDs in water and in different regions such as ODT (hydrophobic) and bare Au (hydrophilic). We used these diffusion barriers in our Kinetic Monte Carlo model to further simulate the alignment phenomenon of the NDs on the bare Au surface patterned with ODT SAMs.

3. RESULTS AND DISCUSSION

Figure 2A is an optical image of a ND suspended droplet on the SAM patterned Au surface. The edge of the drop noticeably suggests that the patterned surface is hydrophobic. By tilting the substrate we were able to move the droplet from one place to another. In fact, it was rather difficult to keep the droplet positioned on top of the SAM patterned Au surface. By tilting or with the help of a pipet we were able to remove the ND droplet from the peripheral areas of the substrate with no residues.

Figure 2B is an optical image of a ND droplet drying; both wet (black region) and dry (blue region with black dots) regions can be seen in the picture. The microscope was focused on the dry region (blue region with black dots) and as such, the

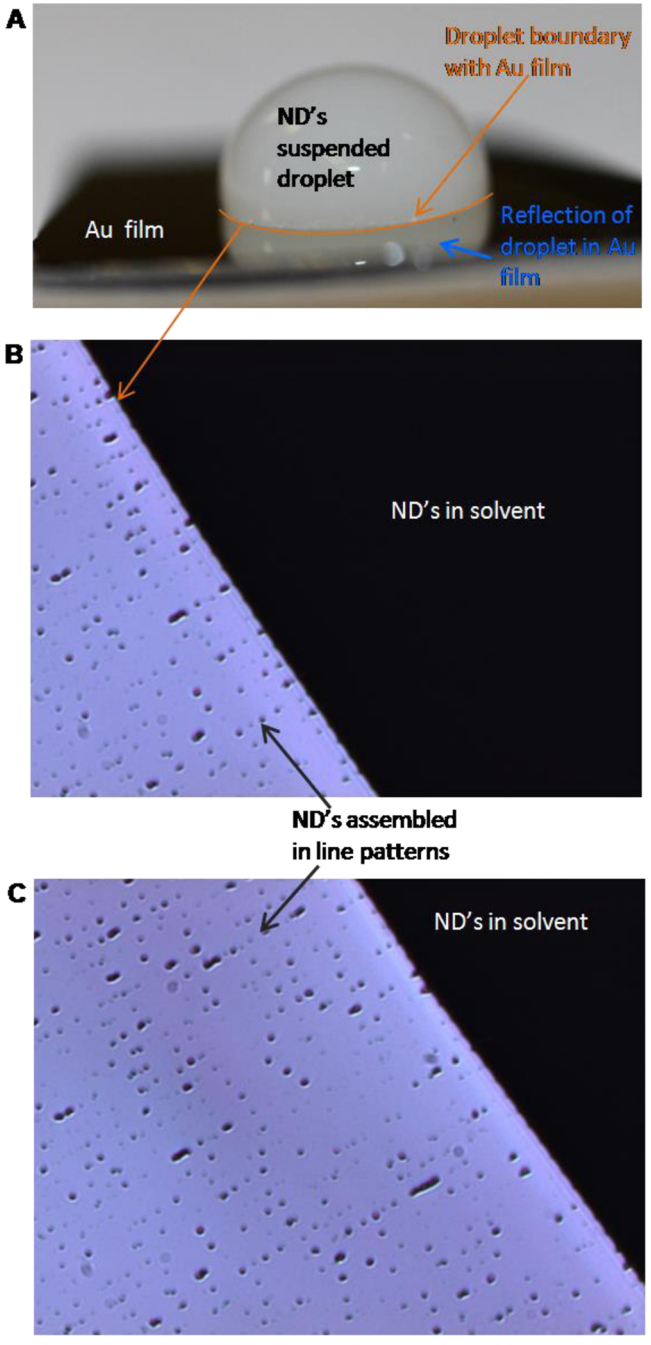

Figure 2. ND droplet on ODT SAM patterned Au thin film and its evaporation behavior at the edge. (A) Optical image of a ND droplet on this Au film. (B) Optical image of the droplet edge; black dots in the blue region are assembled NDs, and the black region is the out of focus part of the droplet. (C) Optical image of the same edge in B after 200 s.

droplet surface (black region) is out of focus. The NDs particles, black dots in blue region, are aligned along straight lines (Figure 2B and C). Figure 2C is an image of same region (Figure 2B) after 200 s. The droplet shrinks with the evaporation of the liquid and leaves the NDs particles along the line patterns, i.e. the bare Au surface regions between the ODT SAMs. We recorded videos of the droplet shrinking process on line/dot SAM patterned surfaces and observed the "release" of NDs along the hydrophilic regions. Furthermore, as the droplet diminished in size, we observed a decrease in droplet shrinking speed and an increase in density of released NDs. This observation can be explained as follows. With the evaporation of liquid, the concentration of NDs increases in the droplet and therefore the density of released NDs particles also increase in the line/dot patterns. These results indicate that solvent evaporation plays an important role in our assembly process and NDs can be assembled in different shapes and sizes according to surface molecular patterns, potentially extending down to the nano scale.[37] In the bottom-up assembly process of NS, the role of the solvent is crucial. We note, however, that in previous reports molecular forces, electrostatic interaction, dielectrophoresis, etc. were believed to play the dominant role in NS assembly.[21−23] Although the importance of solvent shear forces has been addressed in some solvent driven assembly process,[23] only recently has it been reported that the solvent alone can be used to align and assemble some of the NS.[25−30] According to these results[28−30] solvent not only drives the NS into the required region but it is also responsible for the high degree of "crystalinity" within the assembled regions. In such cases, the shape of the assembled NS was controlled by the solvent evaporation processes and explained in-terms of so-called "coffee rings". In these studies, only ring and line shaped assembly has been reported.[25,28−30] Furthermore, NS assembly by lithographically controlled wetting,[26] topographical feature pinning,[25] and capillary forces[27] are very promising, but there is no report about NDs assembly, to best of our knowledge. Our process is thus a flexible route to assemble NDs in any desired architecture. In our NDs assembly process solvent and surface wettability (controlled by the surface chemistry) both play an important role and can be used to assemble NDs in different shapes and geometries at micron- nanoscale. These results are in good agreement with recent observation about CNT assembly.[31,32]

Surface modification with SAMs in this study and previously reported for CNTs and NS assembly are similar.[20−22,24] In those reports, in addition to columbic interaction,[20−22] CNT assembly is solvent driven[24] due to a more favorable energy state in the assembled regions. Closely focusing on the ND-solvent edge in regions containing a SAM pattern, a meniscus is clearly visible during evaporation; bending of solvent toward bare Au region (hydrophilic) in ODT SAM strips (Figure not shown). As the solvent moves backward, it releases the NDs in hydrophilic regions (bare Au stripes) as per the shape of the meniscus.

Similar dynamics were observed when Au surfaces were patterned with ODT SAMs of different shapes. Topographic and lateral force images of SAM patterns were taken by AFM before NDs assembly (Figures not shown). Figure 2B and 2C are the optical images of the aligned NDs where SAM patterns are not visible. To verify that NDs do indeed assemble in bare Au regions within the ODT SAM patterns, we took SEM images. Figure 3A shows the SEM image of assembled NDs in linear regions, of the bare Au surface. The ODT SAM patterns can be seen in Figure 3A (dark gray stripes) match the shape of the PDMS (polydimethylsiloxane) stamp used to create the SAM patterns. They are also consistent with AFM images of SAM patterned surface. Figure 3A shows a SEM image of NDs on an ODT SAM patterned Au surface; NDs are confined exclusively in between ODT-SAM line patterns with sharp, well-defined boundaries that coincide with the ODT boundaries. Even in high density NDs regions, sharp edges are well-defined (Figure 3B). We observed such a high density

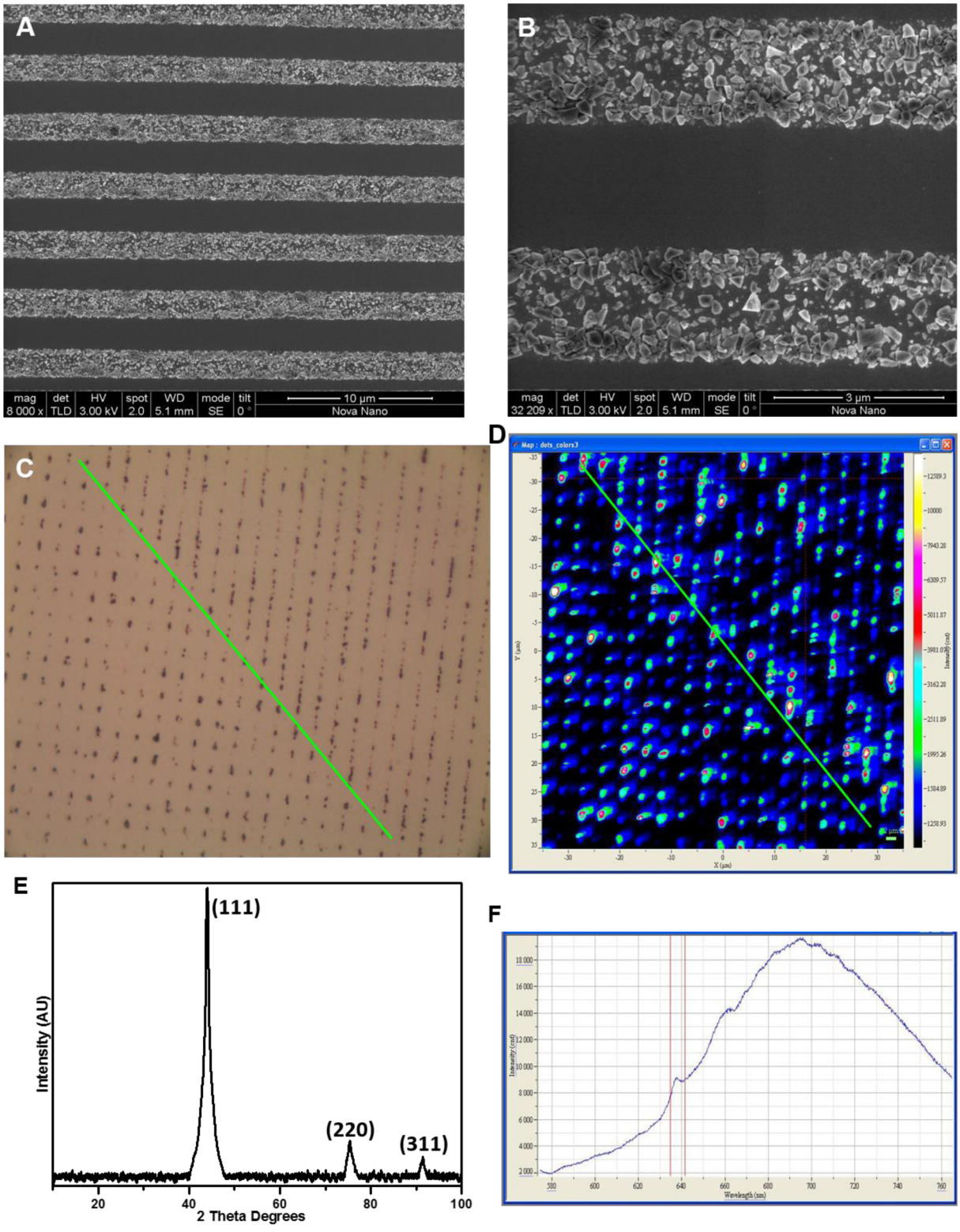

Figure 3. SEM and optical images, PL mapping, and XRD pattern of NDs. (A) SEM image of line patterned NDs. The darker lines are ODT SAMs and the NDs are assembled in between on bare Au surface (bright lines). (B) Closer SEM image of patterned NDs. (C) Optical image of the aligned NDs. The regions below/above the green line are patterned NDs in rectangular/linear patterns. (D) PL spectrum of line and rectangular patterned ND around zero phonon line (ZPL). (E) XRD pattern of NDs. (F) Spectrum from NV's in NDs assembled in parts C and D. The optical image in part C and the PL mapping in part D are of the same region.

of aligned NDs on bare Au strips only when we let the droplet dry to completion over SAM patterned Au surface.

When a patterned substrate dipped in ND solution (very dilute as compare to a ND droplet) for different time intervals, a very low density of assembled NDs was observed in all cases. These results are different from previous reports[20−22] where high densities of assembled NS were obtained from a low concentration NS solution by increasing the dipping time. This

variation could arise from a difference in solvent type—water in the case of ND and dichlorobenzene for CNTs—and needs to be further investigated. However, common to all reports is the fact that no NS assembled in nonwettable, hydrophobic (ODT) regions. ODT SAM was used to create rectangular bare Au regions and NDs assembly was also investigated in these regions; NDs were confined exclusively in between the ODT SAM regions with sharp well-defined boundaries that coincide with the ODT boundaries (optical image Figure 3C: lower half diagonal). These results evidently indicate that the solvent releases the NDs in specific region depending upon the surface chemistry, in particular the wettability of the surface. The latter can be tuned by using SAMs is thus not solely solvent driven as in previous works with "coffee ring" structures.[28−30] Although, substrate−NS interaction plays a role in NS assembly processes;[20−24] however, in our case the role of surface wettability is more prominent and responsible to drive the shape of assembled. It is noteworthy that variation in density of assembled NDs was observed in line/rectangular regions although no empty line/rectangle was observed during several attempts. Controlling the ND concentration in solvent, temperature, and humidity would likely aid to obtaining an equal density of ND in the required regions, though further systematic work is required to benchmark such uniformity.

Our results convincingly show that NDs can be assembled in different shapes on SAM patterned Au surface. Furthermore, methyl terminated SAM patterns can be created on many semiconducting and metallic surfaces[37] therefore suggesting that our assembly process can be used to align NDs on different surfaces. The assembly of NDs on different surfaces in complex shapes, where numbers of NDs can be controlled, could play an important role in developing ND based photonic device. The compatibility of our assembly process with existing micro-/nanofabrication may enable us to optically connect multiple NDs and realize many other device topologies as well.

To verify the optical activity of NV centers in assembled NDs, PL images were taken using a confocal optical microscope and are shown in Figure 3D. For PL mapping, line and dot patterns of ODT SAMs were created on same substrate using two PDMS stamp-patterning steps. Figure 3C is the optical image of the patterned NDs; the left lower-half diagonal is a rectangular pattern and the right upper-half diagonal has line shaped bare Au regions with assembled NDs. For 2D PL image sample with relatively low density of assembled ND was selected to get good spatial resolution. Figure 3D is the 2D PL image generated from the integrated spectral intensity in the 635 nm −642 nm window around the zero phonon line (Figure 3F) of the patterned NDs. PL mapping data convincingly shows that assembled NDs are optically active. PL maps were taken in different regions of the sample and at different intensities as well and similar results were observed. Furthermore, the crystal structure of ND was verified by the XRD pattern, shown in Figure 3E. Intense peaks indexed to the cubic diamond structure; peak position and relative integrated intensities of each peak are well matched with reported diamond peaks.

For potential quantum information applications, it will likely be necessary to couple different NDs optically. Currently it is difficult to fabricate waveguides and cavities in diamond and the growth of diamond in hybrid structures results in polycrystalline diamond with high scattering losses. Approaches where NDs are coupled to microdisks/rings/cavities[38−40] are compatible with our assembly process since it only makes use of standard micro-/nanofabrication processes. In terms of applications to biology, the carboxylic nature of the patterned ND surface can be used to attach specific biological species and their attachment can be detected optically.

4. COMPUTATIONAL RESULTS

4.1. Simulation Details. The model system consists of the Au (111) surface with patterns of the SAM. Using ODT, SAM patterns we created $-CH_3$terminated SAM (hydrophobic) and bare Au (111) surface regions (hydrophilic) on the Au surface. The simulation slab has size 79.94 Å × 86.54 Å × 100 Å. The SAM with tail groups of methyl ($-CH_3$) contains 160 molecules covered with a layer of 2684 water molecules. We used the optimized geometries of these SAMs and a ND particle, which is made up of 32 carbon atoms. The inter- and intramolecular interactions between the water, ND, and SAMs are modeled using the dynamics (ENCAD) force field and energy calculations.[41,42]

A semiempirical tight binding model is used to describe the inter atomic interactions between Au surface atoms.[43] The interactions between the Au surface, water, and the NDs are modeled using the modified Sporh potential.[44] The diffusion pathways and the barriers were calculated by placing the NDs in a cluster of water molecules. The diffusion of the ND species (in water) was explicitly treated by a hopping mechanism in our study. First, we placed the NDs in water in the region which is covered by the ODT SAMs and calculated the diffusion barrier by employing the drag method.[45] Second, we performed the same procedure using the drag method to calculate the NDs diffusion barrier in water on the bare Au (111) surface. On the bare Au (111) surface (hydrophilic regions), the ND has a different barrier as compared to the hydrophobic regions covered with ODT SAMs. The calculated diffusion barriers ($\Delta E_{\mathrm{diff},i}$) for the ND in water in different regions such as hydrophobic and hydrophilic are listed in Table 1. We used these diffusion barriers in our Kinetic Monte Carlo (KMC) model to further simulate the alignment phenomenon of the NDs on the Au (111) surface with patterned ODT SAMs.

Table 1. Calculated Diffusion Barriers of the ND in Water in Different Regions

region	Au (111)	ODT SAM
$\Delta E_{\mathrm{diff},i}$ (eV)	0.130	0.055

The KMC method simulates the time evolution of a system in which possible processes such as diffusion of a species at surfaces or surface reactions with known rates can occur. Details of KMC calculations are available in the Supporting Information.

4.2. Simulation Results. Our results of Kinetic Monte Carlo simulations are shown in Figure 4. These results show a set of three curves representing the fraction of the ND population per unit area as a function of time at different temperatures on Au (111) with patterned SAMs. We started our simulation by randomly covering the patterned Au (111) surface with NDs. In the beginning (at time = 0 s), the population of the NDs per unit area is the same in both regions (hydrophobic and hydrophilic) (Figure 5A). With the passage of time, solvent diffusion comes into play by aligning and pushing the NDs into the hydrophilic regions (bare Au surface regions). Our results show a rapid increase of the ND population in the hydrophilic regions and a rapid decrease of

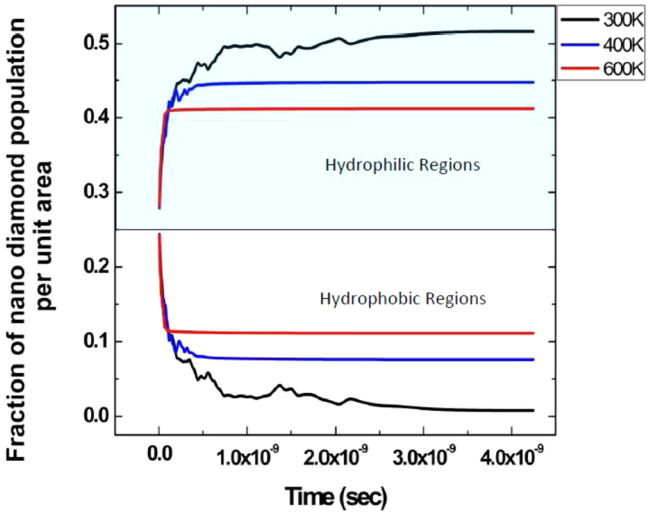

Figure 4. Fraction of ND population (per unit area) on a Au (111) surface covered with patterned SAM as a function of time using KMC simulations.

the population in the hydrophobic regions. These results suggest that the diffusion of NDs in water is faster at the hydrophobic regions and it is slower at the bare Au (111) surface. At 300 K, we see a perfect alignment and confinement of NDs in the hydrophilic (bare Au surface) areas. This can be understood since water desorbs with slower rate at 300 K from the surfaces giving NDs much time to diffuse around at the surface.

In this model, the solvent acts as a catalyst for ND diffusion and it needs to stay at the surface for a sufficient amount of time. We can test this conjecture by running our simulation at higher temperatures where water evaporates quickly. In such a situation, the solvent does not permit NDs to diffuse to the hydrophilic (bare Au surface) areas. Thus, at higher temperatures we cannot see much alignment/confinement of the NDs at the SAM patterned Au (111) surface. Therefore, our theoretical model strongly supports our experimental data suggesting the solvent driven assembly of NDs on the SAM patterned Au surface.

A time evolution of the ND diffusion at the SAM patterned Au (111) surface is shown in Figure 5. Snapshots in Figure 5 were taken respectively at t = 0.0 (A), 1.0 × 10^{-9} (B), 2.0 × 10^{-9} (C), and 4.0 × 10^{-9} s (D). In Figure 5 the blue dots are solvent chunks and red dots are NDs.

5. CONCLUSION

We have demonstrated a robust and flexible strategy for large-scale template directed assembly of NDs, controlled by surface wettability, in arrays of micron size patterns of different shapes. SAM patterns were used to generate textured networks that control the wettability of the patterned regions. Evaporating a droplet of ND in water suspension on the SAM textured surface reliably deposited NDs in hydrophilic (bare Au) regions. Experimental and computational results indicate that

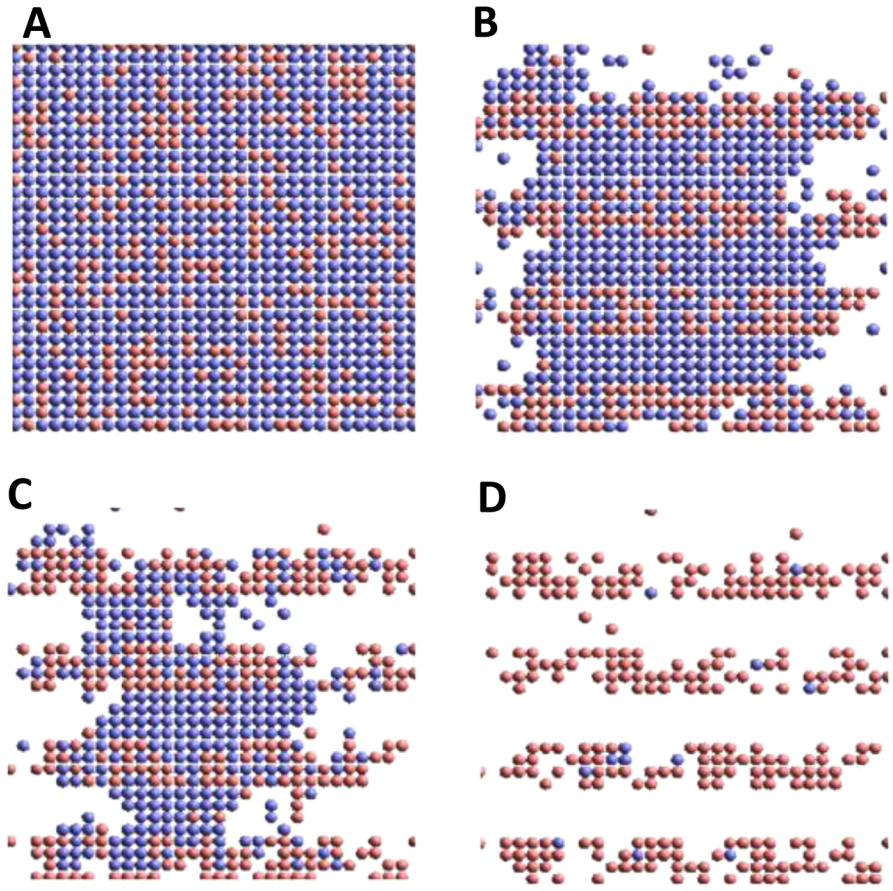

Figure 5. Time evolution KMC simulation of ND diffusion at the SAM patterned Au (111) surface. Snapshots (A) at t = 0.0 s, (B) t = 1.0 × 10^{-9} s, (C) t = 2.0 × 10^{-9} s, (D) t = 4.0 × 10^{-9} s. Blues are solvent chunks and reds are NDs.

the surface wettability controls the path for directed assembly and has the potential to realize elaborate NDs-based devices and hybrid structures. Confocal optical microscopy PL data demonstrated the optical activity of NV centers in the assembled NDs. In light of current interest in producing high-density photonic devices, the simplicity of our technique and its compatibility with standard semiconductor fabrication may open up the door for industrial applications.

■ ASSOCIATED CONTENT

Ⓢ Supporting Information

Information about the Kinetic Monte Carlo methods implemented in our research to simulate the motion and time dependent behavior of nanodiamonds in a solvent drop on the patterned SAM. The kinetics of nanodiamonds in hydrophobic and hydrophilic regions are governed by the interactions between the solvent molecules, nanodiamonds, and the substrate atoms. Such interactions and diffusion energetic are taken to be as in input to our KMC simulations. This material is available free of charge via the Internet at http://pubs.acs.org/.

■ AUTHOR INFORMATION

Corresponding Author

*E-mail: saleemg@kfupm.edu.sa. Phone: +966 3 860 1675. Fax: +966 3 860 2293.

Present Address

○Department of Physics, COMSATS Institute of Information Technology, Islamabad, Pakistan.

Notes

The authors declare no competing financial interest.

■ ACKNOWLEDGMENTS

Support from the KFUPM department of physics is gratefully acknowledged. This work was supported by the Deanship of Scientific Research—King Fahd University of Petroleum and Minerals grant no. RG1103-1,2.

■ REFERENCES

(1) Kubatkin, S.; Danilov, S.; Hjort, M.; Cornil, J.; Brédas, J.-L.; Stuhr-Hansen, N.; Hedegard, P.; Bjørnholm, T. Single-electron Transistor of a Single Organic Molecule with Access to Several Redox States. *Nature* **2003**, *425*, 698−701.

(2) Klein, D. L.; Roth, R.; Lim, A. K.; Alivisatos, A. P.; McEuen, P. L. A. A Single-electron Transistor made from a Cadmium Solenoid Nanocrystals. *Nature* **1997**, *389*, 699−701.

(3) Dietl, T.; Awschalom, D. D.; Kaminska, M.; Ohno, H. *Spintronics (Semiconductor and Semimetals)*, 1st ed; Academic Press: USA, 2008; Vol. 82.

(4) Ohtsu, M. *Progress in Nanophotonics 1*; Springer, 2011.

(5) Yeng, Y. X.; Ghebrebrhan, M.; Bermel, P.; Chan, W. R.; Joannopoulos, J. D.; Soljacic, M.; Celanovic, I. Enabling High-temperature Nanophotonics for Energy Applications. *Proc. Nat. Acad. Sci.* **2012**, *109* (7), 2280−2285.

(6) Strauf, S.; Stoltz, N. G.; Rakher, M. T.; Coldren, L. A.; Petroff, P. M.; Bouwmeester, D. High-frequency Single-photon Source with Polarization Control. *Nat. Photonics* **2007**, *1*, 704−708.

(7) Kurtsiefer, C.; Mayer, S.; Zarda, P.; Weinfurter, H. Stable Solid-State Source of Single Photons. *Phys. Rev. Lett.* **2000**, *85*, 290−293.

(8) Gruber, A.; Drabenstedt, A.; Tietz, C.; Fleury, L.; Wrachtrup, J.; von Borczyshowski, C. Scanning Confocal Optical Microscopy and Magnetic Resonance on Single Defect Centers. *Science* **1997**, *276*, 2012−2014.

(9) Balasubramanian, G.; Neumann, P.; Twitchen, D.; Markham, M. L.; Kolesov, R.; Mizuochi, N.; Isoya, J.; Achard, J.; Beck, J.; Tissler, J.; Jacques, V.; Hemmer, P. R.; Jelezko, F.; Wrachtrup, J. Ultralong Spin Coherence Time in Isotopically Engineered Diamond. *J. Nat. Mater.* **2009**, *8*, 383−387.

(10) Neumann, P.; Kolesov, R.; Naydenov, B.; Rempp, F.; Steiner, M.; Jacqques, V.; Balasubramanian, G.; Markham, M. L.; Twitchen, D. J.; Pezzagna, P.; Meijer, J.; Jelezko, F.; Wrachtrup, J. Quantum Register Based on Coupled Electron Spins in a Room-temperature Solid. *J. Nat. Phys.* **2010**, *6*, 249−253.

(11) Wang, C. F.; Hansan, R.; Awscalom, D. D.; Hu, E. L.; Feygelson, T.; Yang, J.; Butler, J. E. Fabrication and Characterization of Two-dimensional Photonic Crystal Microcavities in Nanocrystalline Diamond. *Appl. Phys. Lett.* **2007**, *91*, 201112.

(12) Rabl, P.; Kolkowitz, S. J.; Koppens, F. H. L.; Harris, J. G. E.; Zoller, P.; Lukin, M. D. A. Quantum Spin Transducer based on Nano Electro-mechancial Resonator Arrays. *Nat. Phys.* **2010**, *6*, 602−608.

(13) Aharonovich, I.; Castelleto, S.; Simpson, D. A.; Su, C.-H.; Greentree, A. D.; Prawer, S. Diamond-based Single-Photon Emitter. *Rep. Prog. Phys.* **2011**, *74*, 076501.

(14) Van der Sar, T.; Heeres, E. C.; Dmochowski, G. M.; de Lange, G.; Robledo, L.; T. H. Oosterkamp, T. H.; R. Hanson, R. Nanopositioning of a Diamond Nanocrystal Containing a Single Nitrogen-vacancy Defect Center. *Appl. Phys. Lett.* **2009**, *94* (17), 173104.

(15) Benson, O. Assembly of Hybrid Photonic Architectures from Nanophotonic Constituents. *Nature* **2011**, *480*, 193−199.

(16) Yoshie, T.; Scherer, A.; Hendrichson, J.; Khitrova, G.; Gibbs, H. M.; Rupper, G.; Ell, C.; Shchekin, O. B.; Deppe, D. G. Vacuum Rabi Splitting with a Single Quantum Dot in a Photonic Crystal Nanocavity. *Nature* **2004**, *432*, 200−203.

(17) Noda, S.; Fujita, M.; Asano, T. Spontaneous-emission Control by Photonic Crystals and Nanocavities. *Nat. photon.* **2007**, *1*, 449−458.

(18) Toyli, D. M.; Weis, C. D.; Fuchs, G. D.; Schenkel, T.; Awschalom, D. D. Chip-scale Nanofabrication of Single Spins and Spin Arrays in Diamond. *Nano Lett.* **2010**, *10*, 3168−3172.

(19) Boudou, J.-P.; Curmi, P. A.; Jelezko, F.; Wrachtrup, J.; Aubert, P.; Sennour, M.; Balasubramanian, G.; Reuter, R.; Thorel, A.; Graffet, E. High yield fabrication of fluorescent nanodiamonds. *Nanotechnology* **2009**, *20* (23), 235602.

(20) Rao, S. G.; Huang, L.; Settawan, W.; Hong, S. Nanotube Electronics: Large-scale Assembly of Carbon Nanotubes. *Nature* **2003**, *25*, 36−37.

(21) Lee, M.; Im, J.; Lee, B. Y.; Myung, S.; Kang, J.; Huang, L.; Kwon, Y.-K.; Hong, S. Linker-free Directed Assembly of High-performance Integrated Devices Based on Nanotubes and Nanowires. *Nat. Nanotechnol.* **2006**, *1*, 66−71.

(22) Heo, K.; Cho, E.; Yang, J.-E.; Kim, M.-H.; Lee, M.; Lee, B. Y.; Kwon, S. G.; Lee, M.-K.; Jo, M.-H.; Choi, H.-J.; Hyeon, T.; Hong, S. Large-scale Assembly of Silicon Nanowire Network-based Devices using Conventional Microfabrication Facilities. *Nano Lett.* **2008**, *8* (12), 4523−4527.

(23) Wang, M. C. P.; Gates, D. D. Directed Assembly of Nanowires. *Mater. Today* **2009**, *12* (5), 34−43.

(24) Wang, Y.; Maspoch, D.; Zou, S.; Schatz, G. C.; Smalley, R. E.; Mirkin, C. A. Controlling the shape, orientation, and linkage of carbon nanotube features with nano affinity templates. *Proc. Nat. Acad. Sci.* **2006**, *103* (7), 2026−2031.

(25) Engel, M.; Small, J. P.; Steiner, M.; Freitag, M.; Greem, A. A.; Hersam, M. C.; Avouris, P. Thin Film Nanotube Transistors Based on Self-assembled, Aligned, Semiconducting Carbon Nanotube Arrays. *ACS Nano* **2008**, *2*, 2445−2452.

(26) Liddle, J. A.; Cui, Y.; Alivisatos, P. Lithographically Directed Self-assembly of Nanostructures. *J. Vac. Sci. Technol., B* **2004**, *22* (6), 3409−3414.

(27) Cavallini, M.; Gentili, D.; Greco, P.; Valle, F.; Biscarini, F. Micro-and Nanopatterning by Lithographically Controlled Wetting. *Nat. Protocols* **2012**, *7* (9), 1668−1676.

(28) Wang, Z.; Bao, R.; Zhang, X.; Ou, X.; Lee, C.-S.; Chang, J. C.; Zhang, X. One-Step Self-Assembly, Alignment, and Patterning of Organic Semiconductor Nanowires by Controlled Evaporation of Confined Microfluids. *Angew. Chem., Int. Ed.* **2011**, *50*, 2811−2815.
(29) Xu, J.; Xia, J.; Lin, Z. Evaporation-Induced Self-Assembly of Nanoparticles from a Sphere-on-Flat Geometry. *Angew. Chem.* **2007**, *119*, 1892−1895.
(30) Han, W.; Lin, Z. Learning from "Coffee Rings": Ordered Structures Enabled by Controlled Evaporative Self-Assembly. *Angew. Chem. Int. Ed.* **2012**, *51* (7), 1534−1546.
(31) Rao, S. G.; Huang, L.; Murray, J. Assembly of Single-walled Carbon Nanotubes on Patterns of Au Nanoparticles. *Appl. Surf. Sci.* **2011**, *258* (1), 1519−1524.
(32) Rao, S. G. Wafer-scale Directed Self-assembly of Nanostructures using Self-assembled Monolayer based Controlled-wetting. *Colloids Surf., A* **2013**, *436*, 1076−1082.
(33) Hanske, C.; Muller, M. B.; Bieber, V.; Tebbe, M.; Jessl, S.; Wittemann, A.; Ferry, A. The Role of Substrate Wettability in Nanoparticle Transfer from Wrinkled Elastomers: Fundamentals and Application toward Hierarchical Patterning. *Langmuir* **2012**, *28*, 16745−16750.
(34) Miele, E.; Malerba, M.; Dipalo, M.; Rondanina, E.; Toma, A.; Angelis, F. D. Controlling Wetting and Self-Assembly Dynamics by Tailored Hydrophobic and Oleophobic Surfaces. *Adv. Mater.* **2014**, DOI: 10.1002/adma.201400310.
(35) Yin, Y.; Lu, Y.; Gates, B.; Xia, Y. Template Associated Self-assembly: A Practical Route to Complex Aggregates of Monodispersed Colloids with Well-defined Sizes, Shapes, and Structures. *J. Am. Chem. Soc.* **2001**, *123*, 8718−8729.
(36) Liu, J.-W.; Liang, H.-W.; Yu, S.-H. Macrosscopic Scale Assembled Nanowire Thin Films and Their Functionalities. *Chem. Rev.* **2012**, *112* (8), 4770−4799.
(37) Love, J. C.; Estroff, L. A.; Kriebel, J. K.; Nuzzo, R. G.; Whitesides, G. M. Self-assembled Monolyers of Thiolates on Metal as a Form of Nanotechnology. *Chem. Rev.* **2005**, *105* (4), 1103−1169.
(38) (a) Park, Y.-S.; Cook, A. K.; Wang, H. Cavity QED with Diamond Nanocrystals and Silica Microspheres. *Nano Lett.* **2006**, *6*, 2075−2079.
(39) Fu, K.-M. C.; Barclay, P. E.; Santori, C.; Faraon, A.; Beausoleil, R. G. Low-temperature tapered-fiber probing of diamond nitrogen-vacancy ensembles coupled to GaP microcavities. *New J. Phys.* **2011**, *13*, 055023.
(40) Riedrich-M?ller, J.; Kipfstuhl, L.; Hepp, C.; Neu, E.; Pauly, C.; Mucklich, F.; Baur, A.; Wandt, M.; Wolff, S.; Fischer, M.; Gsell, S.; Schreck, M.; Becher, C. One- and two-dimensional photonic crystal microcavities in single crystal diamond. *Nat. Nanotechnol.* **2012**, *7*, 69−74.
(41) Levitt, M.; Hirshberg, M.; Sharon, R.; Daggett, V. Potential Energy Function and Parameters for Simulations of the Molecular Dynamics of Proteins and Nucleic Acids in Solution. *Comput. Phys. Commun.* **1995**, *91*, 215−231.
(42) Yang, A.-C.; Weng, C.-I. Influence of Alkanethiol Self-assembled Monolayers with Various Tail Groups on Structural and Dynamic Properties of Water films. *J. Chem. Phys.* **2008**, *129*, 154710.
(43) Rosato, V.; Guillope, M.; Legrand, B. Thermodynamic and Structural Properties of fcc Transition Metal Using a Simple Tight-binding Model. *Philos. Mag. A* **1989**, *59* (2), 321−336.
(44) Dou, Y. S.; Zhigilei, L. V.; Winograd, N.; Garrison, B. J. Explosive Boiling of Water Films Adjacent to Heated Surfaces: A Microscopic Description. *J. Phys. Chem. A* **2001**, *105* (12), 2748−2755.
(45) Rahman, T. S.; Kara, A.; Karim, A.; Al-Rawi, A. Collective Diffusion on Surfaces: Correlation Effects and Adatom Interactions. *NATO Sci. Ser.* 2001, Vol.29, 327−338, Springer, Netherlands.